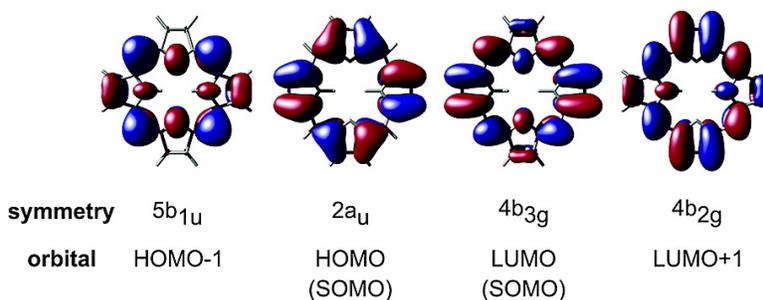Article

The Electronic Structure of the Photoexcited Triplet State of Free-Base (Tetraphenyl)porphyrin by Time-Resolved Electron–Nuclear Double Resonance and Density Functional Theory

Christopher W. M. Kay

symmetry	$5b_{1u}$	$2a_u$	$4b_{3g}$	$4b_{2g}$
orbital	HOMO-1	HOMO (SOMO)	LUMO (SOMO)	LUMO+1

More About This Article

Additional resources and features associated with this article are available within the HTML version:

- Supporting Information
- Links to the 1 articles that cite this article, as of the time of this article download
- Access to high resolution figures
- Links to articles and content related to this article
- Copyright permission to reproduce figures and/or text from this article

View the Full Text HTML

The Electronic Structure of the Photoexcited Triplet State of Free-Base (Tetraphenyl)porphyrin by Time-Resolved Electron–Nuclear Double Resonance and Density Functional Theory

Christopher W. M. Kay*

Contribution from the Institute of Experimental Physics, Free University Berlin, Arnimallee 14, 14195 Berlin, Germany

Received May 22, 2003; E-mail: Chris.Kay@physik.fu-berlin.de

Abstract: The photoexcited triplet states of free-base porphyrin (H_2P) and free-base tetraphenylporphyrin (H_2TPP) have been investigated by time-resolved electron paramagnetic resonance and electron–nuclear double resonance in a toluene glass at 80 K. Both the zero-field splitting parameters, D and E, and the proton A_{zz} hyperfine coupling tensor components could be determined. D is about 13% larger in H_2P than in H_2TPP. In contrast, however, the A_{zz} hyperfine coupling tensor components showed differences of less than 2%. To aid the understanding of these results, the electronic structures of H_2P and H_2TPP have been modeled using density functional theory. The geometrical structures of both molecules in their lowest triplet states were calculated using the Becke3 Lee–Yang–Parr composite exchange correlation functional and the 6-31G* basis set. Hyperfine couplings for these structures were calculated using the same functional but with the extended EPR-II basis set. These allow unambiguous assignment of the experimentally determined couplings. The theoretical values for H_2P and H_2TPP agree with the experimental values in that the presence of the phenyl groups has only a small effect on the unpaired electron spin-density distribution. The difference in sensitivity of the zero-field splitting parameters and the hyperfine couplings to mesophenyl substitution is discussed in terms of the wave functions of the four frontier orbitals of porphyrins introduced by Gouterman.

1. Introduction

Porphyrins and their derivatives are essential cofactors in many biological processes, ranging from light absorption and electron transfer in photosynthesis to oxygen transport and storage in hemoglobin.[1,2] The rich chemistry of the porphyrins stems largely from the nature of the four frontier oribtals HOMO−1, HOMO, LUMO, and LUMO+1, otherwise referred to as Gouterman's four orbitals.[3−5] In metalloporphyrins, the molecule has D_{4h} symmetry, and the two HOMOs and two LUMOs are degenerate. On replacing the central metal ion by two protons, the symmetry is lowered to D_{2h}, and the degeneracy is lifted. However, the energy separations between the HOMO−1 and HOMO and between the LUMO and LUMO+1 are still rather small. Prediction and control of this by, for example, substitution could allow molecules to be designed with the desired photophysical properties in both the ground and the excited states.[4,6,7] Computational results are often compared to spectroscopic data, such as optical absorption,[8] photoelectron,[9,10] and EPR[11−17] (electron paramagnetic resonance) spectra.

Here, we consider the triplet state of free-base porphyrin, H_2P, and tetraphenylporphyrin, H_2TPP, see Figure 1. The former is, at first glance, an ideal model system, but it is difficult to prepare and is rather insoluble. It is, therefore, usually replaced in spectroscopic studies by H_2TPP. The presence of the phenyl groups renders the molecule soluble, but their π systems also overlap, to some extent, with that of the porphyrin moiety. This can be particularly important when one considers the expected degeneracies among the frontier orbitals. The increase in the

(1) Dolphin, D., Ed. *The Pophyrins*; Academic: New York, 1979; Vols. 1−7.
(2) Scheer, H., Ed. *Chlorophylls*; CRC Press: Boca Raton, FL, 1990.
(3) Longuet-Higgins, H. C.; Rector, C. W.; Platt, J. R. *J. Chem. Phys.* **1950**, *18*, 1174−1181.
(4) Gouterman, M. *J. Chem. Phys.* **1959**, *30*, 1139−1161.
(5) Gouterman, M. *J. Mol. Spectrosc.* **1961**, *6*, 138−163.
(6) Ghosh, A. *Acc. Chem. Res.* **1998**, *31*, 189−198.
(7) Nooijen, M.; Bartlett, R. J. *J. Chem. Phys.* **197**, *106*, 6449−6455.
(8) Hashimoto, T.; Choe, Y.-K.; Nakano, H.; Hirao, K. *J. Phys. Chem.* **1999**, *103*, 1894−1904.

(9) Gassman, P. G.; Ghosh, A.; Almlöf, J. *J. Am. Chem. Soc.* **1992**, *114*, 9990−10000.
(10) Gruhn, N. E.; Lichtenberger, D. L.; Hiroshi, O.; Walker, F. A. *Inorg. Chem.* **1999**, *38*, 4023−4027.
(11) van Dorp, W. G.; Soma, M.; Kooter, J. A.; van der Waals, J. H. *Mol. Phys.* **1974**, *28*, 1551−1568.
(12) Fajer, J.; Davis, M. S. In *The Porphyrins*; Dolphin, D., Ed.; Academic: New York, 1979; Vol. IV.
(13) Hamacher, V.; Wrachtrup, J.; von Maltzan, B.; Plato, M.; Möbius, K. *Appl. Magn. Reson.* **1993**, *4*, 297−319.
(14) Kay, C. W. M.; Gromadecki, U.; Törring, J. T.; Weber, S. *Mol. Phys.* **2001**, *99*, 1413−1420.
(15) di Matteo, A.; Di Valentin, M.; Giacometti, G.; Barone, V. *Chem. Phys. Lett.* **2001**, *335*, 427−434.
(16) van Tol, J.; Brunel, L. C.; Angerhofer, A. *Appl. Magn. Reson.* **2001**, *21*, 335−340.
(17) Kay, C. W. M.; Conti, F.; Fuhs, M.; Plato, M.; Weber, S.; Bordignon, E.; Carbonera, D.; Robinson, B. C.; Renner, M. W.; Fajer, J. *J. Phys. Chem. B* **2002**, *106*, 2769−2778.
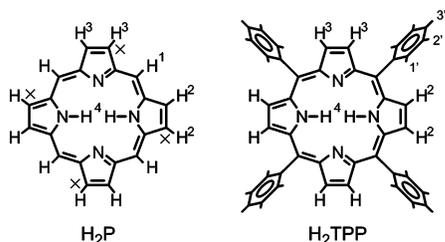
Figure 1. The molecular structures of H_2P and H_2TPP. The proton numbering scheme used in the text is shown. Also shown are crosses marking carbon atoms 3 Å above which point charges were placed in some of the calculations.

number of atoms from 38 in H_2P to 78 in H_2TPP has also posed a great problem for computation, which has only recently been overcome.

Van Dorp and co-workers[11] made the first serious attempt to elucidate the electronic structure and the relative ordering of the four orbitals in the excited triplet state of free-base porphyrin (^3H_2P). Hyperfine couplings (hfcs) measured in single-crystal EPR spectra and assigned to the bridging methine protons (1), see Figure 1, gave a rather large spin density at this position, from which the authors concluded that the HOMO must be the orbital with $5b_{1u}$ symmetry rather than $2a_u$ symmetry. This left open the question as to which orbital was the LUMO. By considering excitations from the orbital with $5b_{1u}$ symmetry to either of the orbitals with $4b_{2g}$ or $4b_{3g}$ symmetry, predicted zfs (zero-field splitting) parameters for both possible excitations could be compared to the experimental values. Thus, the lowest triplet state was assigned as $^3B_{2u}$ ($4b_{3g} \leftarrow 5b_{1u}$).

Later, van der Poel and co-workers[18] performed pulsed-ENDOR (electron−nuclear double resonance) spectroscopy on the central protons (4) of ^3H_2P and noted that there was a symmetry reduction from D_{2h} to C_{2h}, which threw doubt on the earlier assignment. These results were extended by Hamacher and co-workers[13] who performed cw-ENDOR on the excited triplet state of free-base tetraphenylporphyrin (^3H_2TPP) and found that the transition assigned to the α-protons (2) had an unusually large line width that could only be explained by an inequivalence between the two protons, that is, again a reduction from D_{2h} to C_{2h} symmetry. In a time-resolved ENDOR experiment on ^3H_2TPP, we showed that this broad line could actually be resolved into two components.[19] Given that these pairs of protons show reduced symmetry, it follows that the other pair of α-protons (3) should also have nonequivalent hfcs. However, the protons on the phenyl groups also have hfcs, and these obscure those from the latter group of protons in ^3H_2TPP.

Hence, in the present contribution, we have performed time-resolved ENDOR on both ^3H_2TPP and ^3H_2P. Thus, we have been able to resolve the hfcs of the α protons (3) in ^3H_2P and can compare the proton hfcs of both molecules. This is interesting as it has been known for many years that the zfs parameters of H_2TPP are much smaller than those of H_2P.[20,21] It was considered possible that the LUMO and LUMO+1 might be reversed between the two molecules or that some electron density might be delocalized onto the phenyl rings. A more

quantitative interpretation has until the present time not be attempted as the calculation of zfs parameters using either semiempirical or ab initio methods yields only mediocre agreement with experimentally determined values.[17,22−28]

While the zfs parameters represent a global picture of the electron spin distribution in a triplet state, the hfcs map the unpaired electron spin density at magnetic nuclei in the molecule. In contrast to the difficulties in calculating zfs parameters, open-shell DFT (density functional theory) calculations[29,30] using unrestricted self-consistent field (SCF) methods have been developed[31] and used to predict structures and energies of the singlet[32−38] and triplet[14,17,39−41] states of porphyrins. In previous work in this laboratory, we have used the same methods to predict hfcs for the lowest triplet state of porphycene, a structural isomer of porphyrin, and reasonable agreement was found between experiment and theory.[14] Di Matteo and co-workers have also used DFT methods to investigate the properties of the triplet state of quinoxaline, and good agreement was found between theoretical and experimentally determined hyperfine couplings.[15]

Given the difference between the zfs parameters of ^3H_2P and ^3H_2TPP, the immediate question is how do the hfcs in the two molecules compare. As we show using time-resolved ENDOR, these are remarkably similar, a result which DFT calculations were able to reproduce to a good degree. In light of these results, the difference in sensitivity of the zfs and hfcs to the substitution of the phenyl groups in porphyrin is discussed in terms of the four orbital model.

2. Methods

2.1. Experimental. Time-resolved EPR and ENDOR spectra were obtained using a laboratory-built X-band spectrometer consisting of an AEG-20 electromagnet and a Bruker ER041 MR X-band microwave bridge, adapted for transient EPR. After pulsed laser excitation, the EPR and ENDOR signals are directly detected and hence have a nonderivative line shape with A = enhanced absorption, E = emission. A Spectra-Physics Nd:YAG laser (pulse width ≈ 6 ns, wavelength 532 nm, energy/pulse 15 mJ, repetition rate 10 Hz) was used as the light source. The transient signals were detected with a transient recorder (Tektronix TDS 520A). A radio frequency (RF) synthesizer (Hewlett-Packard 8647A) in conjunction with a high-power RF amplifier (ENI A-1000) was used to generate the continuous wave B_2 field in the

(18) van der Poel, W. A. J. A.; Singel, D. J.; Schmidt, J.; van der Waals, J. H. *Mol. Phys.* **1983**, *49*, 1017−1028.
(19) Kay, C. W. M.; Di Valentin, M.; Möbius, K. *Sol. Energy Mater. Sol. Cells* **1995**, *38*, 111−118.
(20) van Dorp, W. G.; Schaafsma, T. J.; Soma, M.; van der Waals, J. H. *Chem. Phys. Lett.* **1973**, *21*, 221−225.
(21) Levanon, H.; Wolberg, A. *Chem. Phys. Lett.* **1974**, *24*, 96−98.

(22) Boorstein, S. A.; Gouterman, M. *J. Chem. Phys.* **1963**, *39*, 2443−2452.
(23) van der Waals, J. H.; ter Maten, G. *Mol. Phys.* **1964**, *8*, 301−318.
(24) Zuclich, J. *J. Chem. Phys.* **1970**, *52*, 3592−3596.
(25) Kooter, J. A.; van der Waals, J. H.; Knop, J. V. *Mol. Phys.* **1979**, *37*, 1015−1036.
(26) Havlas, Z.; Michl, J. *J. Chem. Soc., Perkin Trans. 2* **1999**, 2299−2303.
(27) Bomfleur, B.; Sironi, M.; Raimondi, M.; Vöitlander, J. *J. Chem. Phys.* **2000**, *112*, 1066−1069.
(28) Visser, J.; Groenen, E. J. J. *Chem. Phys. Lett.* **2002**, *356*, 43−48.
(29) Hohenberg, P. C.; Kohn, W. *Phys. Rev. B* **1964**, *136*, 864−871.
(30) Kohn, W.; Sham, L. J. *Phys. Rev. A* **1965**, *140*, 1133−1138.
(31) Pople, J. A.; Nesbet, R. K. *J. Chem. Phys.* **1959**, *22*, 571−572.
(32) Foresman, J. B.; Head-Gordon, M.; Pople, J. A.; Frisch, M. J. *J. Phys. Chem.* **1992**, *96*, 135−149.
(33) Almlöf, J.; Fischer, T. H.; Gassman, P. G.; Ghosh, A.; Häser, M. *J. Phys. Chem.* **1993**, *97*, 10964−10970.
(34) Matsuzawa, N.; Ata, M.; Dixon, D. A. *J. Phys. Chem.* **1995**, *99*, 7698−7706.
(35) Kozlowski, P. M.; Zgierski, M. Z.; Pulay, P. *Chem. Phys. Lett.* **1995**, *247*, 379−385.
(36) Lamoen, D.; Parrinello, M. *Chem. Phys. Lett.* **1996**, *248*, 309−315.
(37) Kozlowski, P. M.; Jarzecki, A. A.; Pulay, P. *J. Phys. Chem.* **1996**, *100*, 7007−7013.
(38) Sundholm, D. *Phys. Chem. Chem. Phys.* **2000**, *2*, 2275−2281.
(39) Nguyen, K. A.; Day, P. N.; Pachter, R. *J. Chem. Phys.* **1999**, *110*, 9135−9144.
(40) Nguyen, K. A.; Pachter, R. *J. Phys. Chem. A* **2000**, *104*, 4549−4552.
(41) Nguyen, K. A.; Day, P. N.; Pachter, R. *J. Phys. Chem. A* **2000**, *104*, 4748−4754.

laboratory-built TM$_{110}$ ENDOR resonator. The temperature was controlled with an Oxford ESR 9 helium continuous-flow cryostat.

H$_2$P was synthesized in the group of J. Fajer (Brookhaven National Laboratory). H$_2$TPP was synthesized in the group of H. Kurreck (Institute of Organic Chemistry, Free University Berlin). Samples in glass capillaries (internal diameter 3 mm) were prepared at a concentration of 5×10^{-4} M in perdeuterated toluene (Aldrich). Oxygen was removed by multiple freeze−pump−thaw cycles under high vacuum conditions. The samples were then sealed.

2.2. Computational. Geometry optimizations of H$_2$P and H$_2$TPP were performed at the unrestricted Kohn−Sham level utilizing the Becke3 hybrid exchange functional[42] combined with the Lee, Yang, Parr correlation functional B3LYP[42,43] as implemented in Gaussian 98,[44] using the 6-31G* basis set.

The DFT calculations of isotropic and dipolar hfcs on the triplet state were performed at the unrestricted Kohn−Sham level using the B3LYP functional. Various basis sets were used, including 6-31G*, 6-31G**, and EPR-II.[45−47] Although the same trends were observed for all of these basis sets, the last gave the best agreement with experiment, so we will restrict our discussion to results from it. In the case of a triplet state, the magnitude of the dipolar hfcs as given by Gaussian 98 had to be divided by 2 so as not to count both unpaired electrons twice.
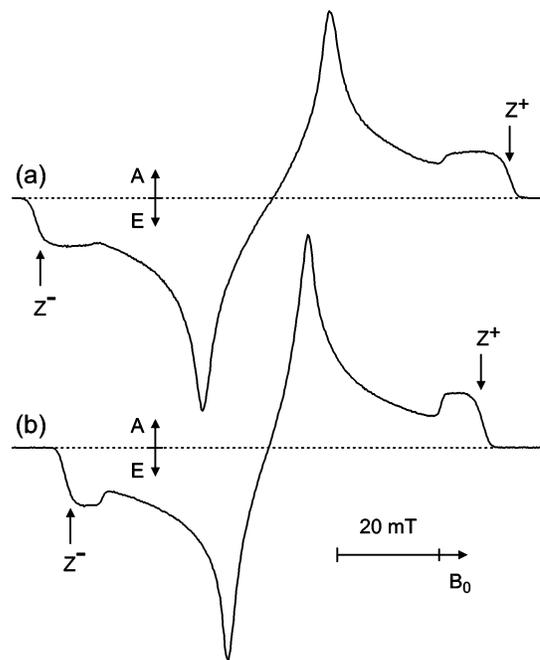
Time-dependent DFT[48] for the calculation of electronic excitation energies and configurations was also performed at the B3LYP/EPR-II level.

The graphical representations of molecular orbitals and iso spin-density surfaces were achieved using the Molden program package.[49]

3. Results and Discussion

3.1. EPR. Figure 2 depicts the time-resolved EPR spectra of ^{3}H$_2$P and ^{3}H$_2$TPP recorded at 80 K. Both spectra show the same EAEAEA polarization pattern. The zfs parameters, $|D| = (46.2 \pm 0.1)$ mT and $|E| = (7.0 \pm 0.1)$ mT, determined from the spectra for ^{3}H$_2$P are in good agreement with values obtained in previous work.[11,20] For ^{3}H$_2$TPP, $|D| = (40.4 \pm 0.1)$ mT and $|E| = (8.3 \pm 0.1)$ mT. These values are again in agreement with literature values.[13,19,21] The absolute signs of D and E are not directly determinable from the spectra, so the modulus is given. The values for D and E from this work together with the literature values are collected in Table 1. The experimental result is that ^{3}H$_2$TPP has a 13% smaller value of D and a 16% larger value of E than ^{3}H$_2$P.

3.2. ENDOR. The molecular, hfc, and zfs z-axes (which are perpendicular to the molecular plane) coincide. Hence, ENDOR experiments performed at the Z$^-$ and Z$^+$ magnetic field positions in the EPR spectrum, see Figure 2, permit measurement of the

(42) Becke, A. D. *J. Chem. Phys* **1993**, *98*, 5648−5652.
(43) Lee, C.; Yang, W.; Parr, R. G. *Phys. Rev. B* **1988**, *37*, 785−789.
(44) Frisch, M. J.; Trucks, G. W.; Schlegel, H. B.; Scuseria, G. E.; Robb, M. A.; Cheeseman, J. R.; Zakrzewski, V. G.; Montgomery, J. A.; Stratmann, R. E.; Burant, J. C.; Dapprich, S.; Millam, J. M.; Daniels, A. D.; Kudin, K. N.; Strain, M. C.; Farkas, O.; Tomasi, J.; Barone, V.; Cossi, M.; Cammi, R.; Mennucci, B.; Pomelli, C.; Adamo, C.; Clifford, S.; Ochterski, J.; Petersson, G. A.; Ayala, P. Y.; Cui, Q.; Morokuma, K.; Malick, D. K.; Rabuck, A. D.; Raghavachari, K.; Foresman, J. B.; Cioslowski, J.; Ortiz, J. V.; Stefanov, B. B.; Liu, G.; Liashenko, A.; Piskorz, P.; Komaromi, I.; Gomperts, R.; Martin, R. L.; Fox, D. J.; Keith, T.; Al-Laham, M. A.; Peng, C. Y.; Nanayakkara, C.; Gonzalez, M.; Challacombe, M.; Gill, P. M. W.; Johnson, B. G.; Chen, W.; Wong, M. W.; Andres, J. L.; Head-Gordon, M.; Replogle, E. S.; Pople, J. A. *Gaussian 98*, revision A.7; Gaussian, Inc.: Pittsburgh, PA, 1998.
(45) Barone, V. *J. Phys. Chem.* **1995**, *99*, 11659−11666.
(46) Barone, V. In *Recent Advances in Density-Functional Methods, Part I*; Chong, D. P., Ed.; World Scientific Publishing: Singapore, 1995.
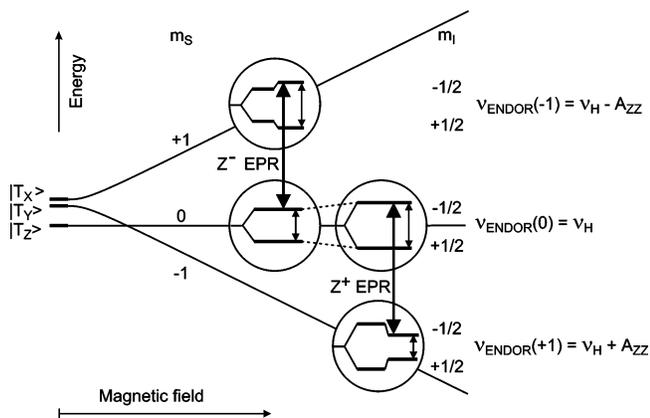(47) Rega, N.; Cossi, M.; Barone, V. *J. Chem. Phys.* **1996**, *105*, 11060−11067.
(48) Stratmann, R. E.; Scuseria, G. E.; Frisch, M. J. *J. Chem. Phys.* **1998**, *109*, 8218−8224.
(49) Schaftenaar, G.; Noordik, J. H. *J. Comput.-Aided Mol. Des.* **2000**, *14*, 123−134.

Figure 2. Time-resolved EPR spectra of (a) ^{3}H$_2$P and (b) ^{3}H$_2$TPP in frozen toluene recorded at 80 K. Integration time window = 0.5−1.5 μs after the laser flash, $P_{mw} = 2$ mW. A and E stand for enhanced absorption and emission, respectively. Z$^-$ and Z$^+$ are the EPR transitions where the z-axis of the zfs tensor is parallel to the external magnetic field. The ENDOR spectra in Figure 4 were recorded at the Z$^-$ magnetic field positions.

Table 1. Comparison of the zfs Parameters D and E of ^{3}H$_2$P and ^{3}H$_2$TPP Derived from the Experiments Described Here with Literature Values^a

molecule	solvent	$|D|$	$|E|$	ref
H$_2$P	toluene	46.2 ± 0.2	7.0 ± 0.2	this work
	n-octane	46.8	7.1	20
H$_2$TPP	toluene	40.4 ± 0.2	8.3 ± 0.2	this work
	ether/ethanol	39.4 ± 0.5	8.8 ± 0.5	21

^{a} All values are given in mT.

A_{zz} hfc tensor component (including sign relative to that of D) of protons in the reference frame of the zfs tensor. The triplet spin energy levels for the z orientation, including first-order hyperfine interaction with one proton, for a molecule with $D > 0$ and $A_{zz} < 0$, are shown in Figure 3. For each EPR transition, there are two ENDOR resonance frequencies at

$$\nu_{\mathrm{ENDOR}}(0) = \nu_{\mathrm{H}} \quad \text{and} \quad \nu_{\mathrm{ENDOR}}(\pm 1) = \nu_{\mathrm{H}} \pm A_{zz} \quad (1)$$

where ν_{H} is the free proton nuclear Larmor frequency. A_{zz} is the sum of an isotropic part (Fermi-contact interaction), A^{iso}, and a dipolar part, A_{zz}^{dip}. A^{iso} is proportional to the spin density in the $2p_z$ orbital of the adjacent carbon or nitrogen atom (McConnell relation),[50] and A_{zz}^{dip} is the integral over the dipolar interactions of the proton spin with the unpaired electron spin distribution over the whole molecule.[51,52] It can be seen from these equations that the resulting ENDOR spectrum is asymmetric, in contrast to the ENDOR spectra of doublet radicals, and, thus, providing that the sign of D is known, the sign of the hfc can also be directly deduced from the spectrum.

(50) McConnell, H. M. *J. Chem. Phys.* **1956**, *24*, 764−766.
(51) Hutchinson, C. A.; Pearson, G. A. *J. Chem. Phys.* **1967**, *47*, 520−533.
(52) Kemple, M. In *Multiple Electron Resonance Spectroscopy*; Dorio, M. M., Freed, J. H., Eds.; Plenum Press: New York, 1979; pp 409−433.

Figure 3. Spin energy levels in the case of the triplet z-axis parallel to the magnetic field, with $D > 0$ and a first-order hyperfine interaction with one proton for $A_{zz} < 0$. The EPR transitions (Z^- and Z^+ EPR) and the ENDOR transitions (ν_{ENDOR}) related to them are indicated by arrows.
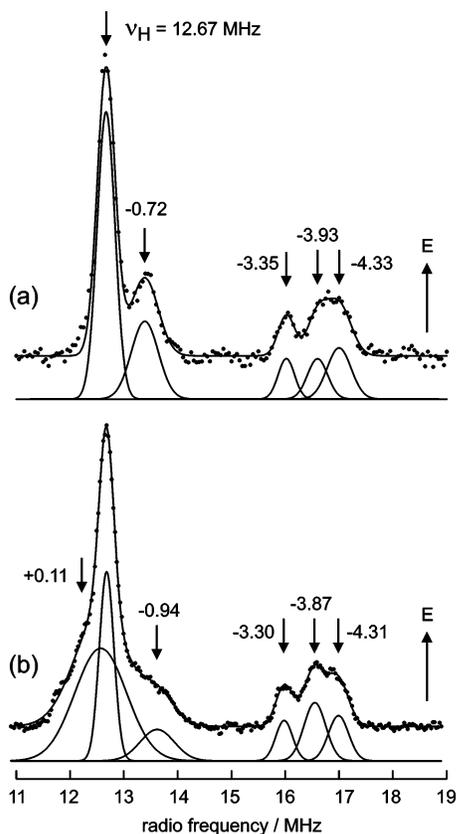
Figure 4. Time-resolved ENDOR spectra of (a) ^{3}H$_2$P and (b) ^{3}H$_2$TPP in frozen toluene recorded at 80 K. Integration time window = 3–10 μs after the laser flash, $P_{mw} = 7.9$ mW, $P_{rf} = 180$ W (2 mT RF field, rotating frame). ν_H indicates the free proton Larmor frequency. The experimental data are indicated by dots, while the drawn line is the best fit obtained using a number of Gaussians which are also shown, vertically shifted for clarity.

The time-resolved ENDOR spectra of ^{3}H$_2$P and ^{3}H$_2$TPP, obtained at 80 K at the Z$^-$ magnetic field positions in Figure 2, are shown in Figure 4. Because the Z$^-$ transition in the EPR spectra is spin-polarized in emission, the ENDOR spectra are also spin-polarized in emission. For the convenience of the reader, the spectra have been inverted.

The main intensity at ν_H stems from transitions in the $m_S = 0$ manifold. This is common to all protons and thus dominates the spectrum. The other ENDOR transitions appear at frequen-

cies greater than ν_H. Given that D is positive as expected for aromatic planar molecules,[53] then inspection of the spectra shows that the A_{zz} hfc tensor components are negative, see eq 1. Deconvolution of the ENDOR spectra was achieved with the computer program Matlab (The Math Works, Inc.) using an appropriate number of Gaussian lines added together. The individual contributions and the final fits are shown together with the experimental data in Figure 4. The A_{zz} values are collected in Table 2, together with literature values for ^{3}H$_2$P[11,18] and ^{3}H$_2$TPP.[13,19] The hfcs of ^{3}H$_2$TPP are all very slightly smaller than those of ^{3}H$_2$P, but in contrast to the zfs parameters the differences are under 2%.

The spectral feature at $\nu_H + 3.3$ MHz has previously been assigned by selective deuteration[13] of ^{3}H$_2$TPP to the N–H protons (4). Assignment of the other hfcs follows previous work using semiempirical molecular orbital calculations[13] and is confirmed by the DFT calculations given in section 3.4. The broad feature around $\nu_H + 4$ MHz, which can be fitted with two Gaussian lines centered at $\nu_H + 3.9$ MHz and $\nu_H + 4.3$ MHz, belongs to the α-protons (2) on the imine pyrrole rings. In the ^{3}H$_2$P spectrum, the α-protons (3) on the azomethine pyrrole rings can now be assigned to the narrow but intense feature at $\nu_H + 0.7$ MHz. These assignments are supported by comparing the integrals of each set of transitions, which should be proportional to the number of contributing protons. Thus, the transition assigned to the four α-protons (3) has approximately the same area as the doublet assigned to the four α-protons (2), whereas the area under the transition assigned to the two N–H protons (4) is about half the size. In the ^{3}H$_2$-TPP spectrum, the line due to the α-protons (3) on the azomethine pyrrole rings is obscured by the broad feature due to the phenyl protons, which appear in the range $+0.11 > \nu_H > -0.94$ MHz. The increased spectral resolution in the ^{3}H$_2$P spectrum allows a more precise determination of the hfcs, which is important for a discussion of the electronic structure.

3.3. Structure Optimizations. The structure of ^{3}H$_2$P is identical to that calculated by Nguyen and Pachter[40] with B3LYP/6-31G(d), but different from that given by the same authors previously.[39] Our structure shows small differences from the singlet ground-state structure calculated using DFT methods.[32–37] The porphyrin moiety of ^{3}H$_2$TPP is essentially identical to that of ^{3}H$_2$P, and the phenyl rings make a dihedral angle with the porphyrin plane of 67.8°, which is close to the angle given by X-ray crystallography.[54]

3.4. HFC Calculations. A comparison of spin densities in the triplet state with those in the cation and anion radicals can be made in the approximation that the triplet π density on the i-th carbon atom is the average of the π density on the cation and anion:[55]

$$\rho_T(C_i) = [\rho_C(C_i) + \rho_A(C_i)]/2 \qquad (2)$$

In the approximation that the same McConnell factors Q are valid for the triplet state, the radical cation, and the anion,[55] then the isotropic triplet hfcs are given by:

$$A_T^{iso} = (A_C^{iso} + A_A^{iso})/2 \qquad (3)$$

(53) Hornig, A. W.; Hyde, J. S. *Mol. Phys.* **1963**, *6*, 33−41.
(54) Silvers, S. J.; Tulinsky, A. *J. Am. Chem. Soc.* **1967**, *89*, 3331−3337.
(55) Carrington, A.; McLachlan, A. D. *Introduction to Magnetic Resonance*; Harper International: New York, 1969.

Table 2. A_{zz} Proton hfc Components of ^3H_2P and ^3H_2TPP As Derived from the Time-Resolved ENDOR Experiments Shown in Figure 4[a]

molecule			proton position			
	1	phenyl	2	3	4	ref
H$_2$P	n.d.		−3.93/−4.33	−0.72	−3.35	this work
	n.d.		n.d.	n.d.	−3.28/3.04	18
	11.0 ± 0.6[b]		n.d.	n.d.	n.d.	11
H$_2$TPP		+0.11 < A < −0.94	−3.87/−4.31	n.d.	−3.30	this work
		+0.6 ± 0.2	−3.9/−4.3	−0.7/−1.0	−3.2	19
		+0.7 ± 0.2	−3.9	−0.8/−1.4	−3.2	13

[a] Estimated errors ±0.02 MHz. The magnitudes and the signs were determined as described in the text. Assignments are made by a comparison with the theoretical values for the respective triplet states given in Table 3. For comparison, hfcs derived from previous studies are also shown. [b] This coupling is derived from single-crystal EPR experiments and corresponds to A^{iso}, not A_{zz}.

Table 3. Comparison of A^{iso} hfc Tensor Components of the Cation Radical, Anion Radical, and Triplet State of H$_2$P[a]

proton	cation	anion	(cation + anion)/2	triplet
1	−17.87	−10.90	−14.38	−13.35
2	−0.58	−6.67	−3.62	−3.68
3	+1.43	+0.42	+0.92	+0.72
4	−4.52	+0.46	−2.03	−1.83

[a] The values were calculated at the unrestricted B3LYP/EPR-II level using structures optimized in the triplet state at the unrestricted B3LYP/6-31G* level. All values are given in MHz.

Table 4. Comparison of A_{zz}^{dip}, A_{iso}, and A_{zz} hfc Tensor Components of ^3H_2P and ^3H_2TPP[a]

molecule	position	A_{zz}^{dip}	A^{iso}	A_{zz}
H$_2$P	1	−0.88	−13.35	−14.23
	2	−1.01	−3.68	−4.69
	3	−0.73	0.72	−0.01
	4	−2.71	−1.83	−4.54
H$_2$P including charges	1	−0.94	−13.34/−13.70	−14.28/−14.64
	2	−0.96/−1.01	−3.32/−3.83	−4.28/−4.84
	3	−0.74/−0.76	0.70/0.73	−0.04/−0.03
	4	−2.71	−1.86	−4.57
H$_2$TPP	phenyl 1		−0.95	
	phenyl 2		0.74	
	phenyl 3		−0.60	
	2	−0.95	−3.40	−4.35
	3	−0.71	0.71	0.00
	4	−2.56	−1.82	−4.38

[a] The values were calculated at the unrestricted B3LYP/EPR-II level using structures optimized in the triplet state at the unrestricted B3LYP/6-31G* level. The components calculated for H$_2$P including charges were performed in the presence of four point charges placed 3 Å above the porphyrin plane, as indicated by crosses in Figure 1. For the protons on the phenyl rings only A^{iso} values are given, as the principal axes of the A^{dip} hfc tensor components are not parallel to the molecular axes. In the case of a triplet state, the magnitude of A_{zz}^{dip}, given in the output of Gaussian 98, had to be divided by 2 not to count both unpaired electrons twice. All values are given in MHz.

where the subscripts T, C, and A refer to triplet, cation, and anion, respectively. Using the optimized structure of ^3H_2P, we have, therefore, calculated the isotropic hfcs for the cation, anion, and triplet states, to test the validity of this relationship in the case of ^3H_2P. The isotropic hfcs for the three states are given in Table 3.

It can be seen that the expected relationship between the average of the cation and anion isotropic hfcs and those for the triplet state is followed, giving us confidence that the DFT method is suited to the calculation of hfcs for systems with $S = 1$.
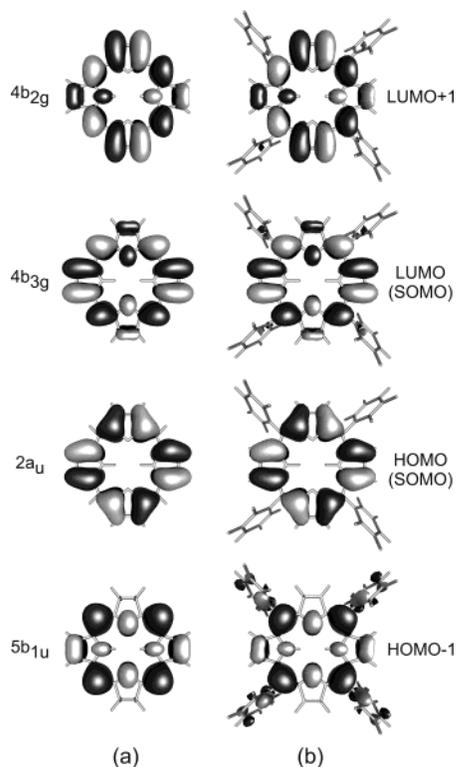
In Table 4, the calculated A_{zz}^{dip}, A_{iso}, and A_{zz} hfc tensor components of ^3H_2P and ^3H_2TPP are presented. All values for ^3H_2TPP are slightly smaller than those for ^3H_2P, in agreement with experiment. The calculations predict the correct trend and

allow the individual hfcs to be assigned. Thus, the α-protons (3) on the azomethane pyrrole rings have small hfcs, while those on the imine rings (2) have larger hfcs. The N−H protons (4) also have significant hfcs. However, the actual agreement is not so good, with the spread of calculated hfcs being larger than the experimental values. This overestimation is also true for the isotropic hfc for the methine protons (1) which were determined by van Dorp and co-workers from single-crystal EPR measurements to be 11 ± 0.6 MHz,[11] whereas the calculations give −13.35 MHz.

An intriguing question arising from the ENDOR spectra is why the ENDOR transitions from the α-protons (3) on the azomethine pyrrole rings and N−H protons (4) have small line widths, while the α-protons (2) on the imine pyrrole rings are broadened into a doublet. The nonequivalence of these protons indicates a symmetry reduction from D_{2h} to C_{2h} in both ^3H_2P and ^3H_2TPP as reported earlier.[13,18,19] To our knowledge, the origin of this effect has not been examined in detail. Here, we consider the possibility that a symmetry reduction occurs due to π-stacking. With toluene as the solvent, however, interporphyrin π−π-stacking is significantly reduced because the solvent competes for the optimum π-stacking positions.[56] Indeed, we have previously reported that H$_2$TPP and free-base tetraphenylchlorin are macroscopically ordered in the crystalline phase of toluene[19,57] so there are certainly ordering forces at work. Hence, π-stacking of the porphyrin and toluene molecules should be considered. There are a plethora of possibilities to be considered ranging from perpendicular to coplanar offset confirmations.[58−61] The geometries are thought to be controlled by a balance between attractive interaction between the π-electrons and the σ framework and repulsive π−π interactions. From both X-ray crystallography and model calculations, it is clear that the interplanar distances between aromatic rings are typically in the range 3−4 Å.[58−62]

A full analysis of such effects are beyond the scope of this paper, but to try to gain a qualitative understanding of their influence, we have repeated the DFT calculations for ^3H_2P including four positive charges placed 3 Å above the porphyrin ring at the positions indicated by crosses in Figure 1. This

(56) Sanders, G. M.; van Dijk, M.; van Veldhuizen, A.; van der Plas, H. C.; Hofstra, U.; Schaafsma, T. J. *J. Org. Chem.* **1988**, *53*, 5272−5281.
(57) Kay, C. W. M.; Di Valentin, M.; Möbius, K. *J. Chem. Soc., Perkin Trans. 2* **1997**, 2563−2568.
(58) Hunter, C. A.; Sander, J. K. M. *J. Am. Chem. Soc.* **1990**, *112*, 5525−5534.
(59) Hobza, P.; Selzle, H. L.; Schlag, E. W. *J. Phys. Chem.* **1996**, *100*, 18790−18794.
(60) Tsuzuki, S.; Honda, K.; Uchimaru, T.; Mikami, M.; Tanabe, K. *J. Am. Chem. Soc.* **2002**, *124*, 104−112.
(61) Tsuzuki, S.; Honda, K.; Azumi, R. *J. Am. Chem. Soc.* **2002**, *124*, 12200−12209.
(62) Robinson, B. C.; Barkigia, K. M.; Renner, M. W.; Fajer, J. *J. Phys. Chem. B* **1999**, *103*, 7324−7328.

Figure 5. Gouterman's four orbitals for (a) ^3H_2P and (b) ^3H_2TPP at an electron density value of 0.02 e/au^3. Note that in the triplet state both the HOMO and the LUMO are SOMOs. The dark and light areas denote regions of opposite sign of the wave function.

Table 5. Energies for Gouterman's Four Orbitals of Ground-State H_2P, ^3H_2P, and $^3H_2TPP^a$

orbital	symmetry	^3H_2TPP	^3H_2P	^1H_2P	$^1H_2P^{36}$	$^3H_2P^{39}$
LUMO+1	$4b_{2g}$	−2.45	−2.51	−2.36	−1.94	−2.21
LUMO	$4b_{3g}$	−3.74	−3.89	−2.73	−1.92	−2.23
HOMO	$2a_u$	−5.59	−5.74	−5.64	−4.15	−5.28
HOMO−1	$5b_{1u}$	−5.73	−6.14	−5.31	−3.90	−5.13

^{a}These were calculated at the unrestricted B3LYP/EPR-II level using structures optimized in the triplet state at the unrestricted B3LYP/6-31G* level. Comparison with literature values calculated for ground-state H_2P^{36} and $^3H_2P.^{39}$ Note that the labels HOMO and LUMO only apply to our calculations for the triplet state, whereas the symmetry labels apply to all. All values are given in eV.

The electron−electron dipolar interaction arises predominantly from single excitations involving the frontier orbitals, such as (LUMO ← HOMO) and (LUMO+1 ← HOMO−1). To see if there is any significant contribution of the latter excitation, we have also performed time-dependent DFT calculations on both ^3H_2P and ^3H_2TPP to determine what is the main configuration of the lowest triplet state in these molecules. For ^3H_2P, the main configuration is 0.88521(LUMO ← HOMO) − 0.24380(LUMO+1 ← HOMO−1) + 0.13593(LUMO+2 ← HOMO−8), while for ^3H_2TPP it is 0.89447(LUMO ← HOMO) + 0.22671(LUMO+1 ← HOMO−1) − 0.10911(LUMO+2 ← HOMO−16). The calculations show that the (LUMO ← HOMO) excitation is the dominant one, but that there is a significant contribution from the (LUMO+1 ← HOMO−1) excitation. Thus, we can qualitatively conclude that the reduction of the zfs in ^3H_2TPP derives from the contribution of the (LUMO+1 ← HOMO−1) excitation to the triplet wave function.

Van Dorp and co-workers concluded that the lowest triplet state is $^3B_{2u}$ corresponding to an excitation from a $5b_{1u}$ symmetry HOMO to $4b_{3g}$ symmetry LUMO.[11] Our calculations agree with the LUMO assignment but not with the HOMO, which is switched to the $2a_u$ symmetry orbital. Nevertheless, the energy separation between the HOMO and HOMO−1 orbitals is small, and the relative ordering of the energy levels proves critically dependent on the method of calculation and the spin state, see Table 5, for a comparison of literature values with our own. Thus, we find that between ^3H_2P and H_2P the ordering of the HOMO and HOMO−1 is reversed. This is in agreement with the result of Lamoen and Parrinello who calculated the singlet ground state using a local density approximation method.[36]

With the pictorial representation of the molecular orbitals, we can also qualitatively explain why the hfcs from the α-protons (2) split under the influence of an asymmetric pseudoenvironment, while the α-protons (3) do not. In the $4b_{3g}$ symmetry LUMO, the wave function at the carbon has a different sign for each of the pairs of imine protons (2), while for the pairs of azomethane protons (3) it has the same sign. Hence, a larger differentiating effect is expected for the former than for the latter. In the other occupied orbitals of $2a_u$ and $5b_{1u}$ symmetry, the wave function at the carbon has either the same or the opposite sign for the pairs of protons, and hence no differentiating effect is expected.

4. Conclusions

The nature of the paramagnetic triplet state of two free-base porphyrins has been investigated by magnetic resonance and theoretical techniques. The experiments allowed both zfs and hfcs to be determined. The substitution of phenyl groups into

mimics an asymmetric environment and lowers the symmetry of H_2P from D_{2h} to C_{2h}, thus breaking the equivalence of the two pairs of α-protons (2) and (3). This simple model may be taken to represent the charges due to toluene protons and lets us avoid the pitfalls of attempting to precisely calculate optimal π-stacking configurations, which even with state-of-the-art theoretical methods is not facile.[59−61]

The result of the calculation, presented in Table 4, is that the hfcs for the pairs of otherwise equivalent protons are now different, but the differences are not the same. The hfcs for α-protons (2) on the imine rings show a spread of 0.5 MHz, while the α-protons (3) on the azomethine rings and the N−H protons (4) are hardly affected. This models the effect observed in the ENDOR spectrum: a symmetry reduction which appears to only affect one pair of protons. To understand this result, we have to consider the symmetries of the molecular orbitals, which we will now do.

3.5. Molecular Orbitals. In Figure 5, we present the four frontier orbitals calculated at the unrestricted B3LYP/EPR-II level for (a) ^3H_2P and (b) ^3H_2TPP. Although in the triplet state both HOMO and LUMO are SOMOs, we retain the ground-state labeling for clarity. The wave functions of the two molecules are rather similar, as expected from the ENDOR data and hfc calculations. There is no indication of a change in orbital ordering, although the HOMO to HOMO−1 gap is significantly reduced in ^3H_2TPP with respect to ^3H_2P, see Table 5. A further significant difference is that the HOMO−1 in ^3H_2TPP has considerable electron density on the phenyl groups, whereas the other orbitals are effectively unchanged. This is important for an understanding of why the zfs is smaller in ^3H_2TPP than in ^3H_2P.

free-base porphyrin had a dramatic effect on the former, while the latter were almost unaffected. The hfcs showed that the symmetry is indeed reduced from D_{2h} to C_{2h}, although particular positions in the molecule were more strongly affected than others.

In contrast to previous EPR data on variously substituted metalloporphyrin π cation radicals,[12,63] the hyperfine data presented here do not suggest that the HOMO switches from $2a_u$ and $5b_{1u}$ symmetry when going from ^3H_2P to mesosubstituted ^3H_2TPP. Possibly the situation is different in triplet states as compared to cation and anion radicals, but perhaps more importantly the higher symmetry (D_{4h}) of metalloporphyrins means that the two HOMOs and two LUMOs are formally degenerate. Thus, metalloporphyrins are necessarily much more sensitive to substitutions that change the relative energies of the frontier orbitals. It would, therefore, be interesting to compare the electronic wave functions of the triplet states of mesosubstituted and nonsubstituted metalloporphyrins by EPR and ENDOR.

The experimentally determined hfcs for the two molecules were very similar, as were the hfcs predicted using DFT methods, although the quantitative agreement between experiment and theory was not so good. The lack of effect on the hfcs by phenyl-substitution can be understood in terms of the mechanism of spin polarization. Isotropic hfcs arise from s-spin density, not from p- or π-spin density. Hence, hfcs are less sensitive to changes such as substitution as electrons in all orbitals contribute, including those in the core orbitals which are better shielded from external influences. On the other hand, the well-known sensitivity of the zfs to environmental effects[64,65] can be understood in that it is largely the frontier orbitals which contribute to this interaction. These are perturbed by neighboring atoms or by small changes in the molecule itself, such as substitution.

To gain some physical insight into solvent−solute interactions, which could be responsible for lowering molecular symmetry, we have taken a simple model whereby point changes were introduced 3 Å above the porphyrin plane. The DFT calculations showed that the effect on the proton hfcs was not uniform. Rather, it depended on the nature of the molecular orbital at the heavy atom to which the proton was attached. Thus, hfcs from otherwise equivalent protons may be expected to differ for some positions in a molecule but not for others, as was indeed observed in the ENDOR experiments. Future work should employ more realistic models using high-resolution X-ray crystallography structures, DFT calculations, and ENDOR spectroscopy to explore this important area − solute−solvent or cofactor−protein interactions − in a more quantitative manner.

Time-resolved EPR allows the zfs parameters and the spin-polarization pattern of the triplet state to be determined. The latter cannot be unambiguously determined by cw-EPR, due to the admixture of spin-polarized and Boltzmann signals. Time-resolved ENDOR allows the hyperfine interaction of the unpaired electrons with magnetic nuclei to be determined even for species with lifetimes in the microsecond range. Thus, a combination of magnetic resonance and the powerful theoretical methods now available yields precious information on the triplet wave function. This is essential if a deeper understanding of the nature of excited states in biological and artificial systems is to be attained.

JA036278J

(63) Fajer, J.; Borg, D. C.; Forman, A.; Adler, A. D.; Varedi, V. *J. Am. Chem. Soc.* **1974**, *96*, 1238−1239.
(64) Thurnauer, M. C. *Rev. Chem. Intermed.* **1979**, *3*, 197−229.
(65) Budil, D. E.; Thurnauer, M. C. *Biochim. Biophys. Acta* **1991**, *1057*, 1−41.